J Physiol 588.2 (2010) pp 325–339

The Journal of Physiology

Atrial natriuretic peptide modulation of albumin clearance and contrast agent permeability in mouse skeletal muscle and skin: role in regulation of plasma volume

Fitz-Roy E. Curry[1], Cecilie Brekke Rygh[2,4], Tine Karlsen[2,4], Helge Wiig[2], Roger H. Adamson[1], Joyce F. Clark[1], Yueh-Chen Lin[1], Birgit Gassner[3], Frits Thorsen[2], Ingrid Moen[2], Olav Tenstad[2], Michaela Kuhn[3] and Rolf K. Reed[2]

[1]*Department of Physiology and Membrane Biology, School of Medicine University of California, Davis, CA, USA*
[2]*Department of Biomedicine, University of Bergen, Bergen, Norway*
[3]*Institute of Physiology, University of Würzburg, Würzburg, Germany*
[4]*Heart and Circulatory Group, Haukeland University Hospital, Bergen, Norway*

Atrial natriuretic peptide (ANP) via its guanylyl cyclase-A (GC-A) receptor participates in regulation of arterial blood pressure and vascular volume. Previous studies demonstrated that concerted renal diuretic/natriuretic and endothelial permeability effects of ANP cooperate in intravascular volume regulation. We show that the microvascular endothelial contribution to the hypovolaemic action of ANP can be measured by the magnitude of the ANP-induced increase in blood-to-tissue albumin transport, measured as plasma albumin clearance corrected for intravascular volume change, relative to the corresponding increase in ANP-induced renal water excretion. We used a two-tracer method with isotopically labelled albumin to measure clearances in skin and skeletal muscle of: (i) C57BL6 mice; (ii) mice with endothelium-restricted deletion of GC-A (floxed GC-A × tie2-Cre: endothelial cell (EC) GC-A knockout (KO)); and (iii) control littermates (floxed GC-A mice with normal GC-A expression levels). Comparison of albumin clearances in hypervolaemic EC GC-A KO mice with normovolaemic littermates demonstrated that skeletal muscle albumin clearance with ANP treatment accounts for at most 30% of whole body clearance required for ANP to regulate plasma volume. Skin microcirculation responded to ANP similarly. Measurements of permeability to a high molecular mass contrast agent (35 kD Gadomer) by dynamic contrast-enhanced magnetic resonance imaging (DCE-MRI) enabled repeated measures in individual animals and confirmed small increases in muscle and skin microvascular permeability after ANP. These quantitative methods will enable further evaluation of the contribution of ANP-dependent microvascular beds (such as gastro-intestinal tract) to plasma volume regulation.

(Received 18 August 2009; accepted after revision 24 November 2009; first published online 30 November 2009)
Corresponding author F. E. Curry: Department of Physiology and Membrane Biology, School of Medicine, 1 Shields Avenue, University of California, Davis, Davis, CA 95616, USA. Email: fecurry@ucdavis.edu

Abbreviations ANP, atrial natriuretic peptide; BW, body weight; EC, endothelial cell; DCE-MRI, dynamic contrast-enhanced magnetic resonance imaging; GC-A, guanylyl cyclase-A; HSA, human serum albumin; KO, knockout; MR, magnetic resonance; MRI, magnetic resonance imaging; P_s, solute permeability coefficient; PS, permeability–surface area product; ROI, region of interest.

Introduction

The aim of these experiments was to test further the hypothesis that atrial natriuretic peptide (ANP) modulates plasma volume by preferentially regulating the permeability of vascular endothelium. These experiments were designed to follow up the experiments of Sabrane and colleagues who demonstrated that mice with endothelial (EC) restricted deletion of the guanylyl cyclase A (GC-A) receptor for ANP (EC GC-A KO mice) had expanded vascular volumes and were hypertensive in spite of normal renal function and vasodilatation in response to ANP (Sabrane *et al.* 2005). Furthermore, the acute hypovolaemic action of ANP was abolished in EC GC-A KO mice. As part of detailed comparisons of renal and cardiovascular functions between knockout and control

DOI: 10.1113/jphysiol.2009.180463

genotypes, Sabrane *et al.* (2005) used a single tracer method to measure the ANP-induced accumulation of isotopically labelled albumin in various mouse tissues and demonstrated that albumin accumulation was reduced in the EC GC-A KO mice to close to 50% of values in control littermates in skeletal muscle and gastro-intestinal (GI) tissue, but to a lesser extent (to an average of 80% of control) in other tissues including heart, lung, kidney, spleen and liver. These observations, as well as more recent direct measurements using fluorescently labelled albumin in a skin fold chamber preparation in the same mice, were consistent with a role for ANP as a regulator of vascular endothelial permeability (Schreier *et al.* 2008). However, as noted in the original paper and in an accompanying commentary, these investigations were not designed to estimate the magnitude of vascular permeability coefficients in different tissues and to take into account potential changes in the vascular volumes and surface area for exchange for albumin in response to ANP (Curry, 2005; Sabrane *et al.* 2005). Thus, one goal of the present study was to determine the specific contribution of ANP-modulated vascular permeability to macromolecules, particularly albumin, to the re-distribution of plasma protein and water between the vascular and extravascular space to regulate plasma volume.

One test to study the role of ANP as an endothelium-dependent regulator of vascular volume is to compare the renal excretion of water (which concentrates plasma proteins) with blood-to-tissue clearance of plasma proteins (which reduces plasma protein concentration). To do this we compared the rate that plasma proteins exchange from plasma to interstitial space with the rate that plasma proteins are concentrated in the plasma as a result of ANP-dependent renal excretion of water (Trippodo & Barbee, 1987; Renkin & Tucker, 1996). This test is explained in the Discussion and Appendix 1 using a mass balance and previous results to measure interstitial fluid volumes, renal water excretion and albumin clearances in rat models of ANP action. The availability of the EC GC-A KO transgenic mice and their littermate controls enables this test. Previously the most detailed investigations of these mechanisms were carried out by Renkin and colleagues (Tucker *et al.* 1992; Renkin & Tucker, 1996, 1998). These investigators employed a two-tracer method using albumin labelled with ^{131}I and ^{125}I to enable measurement of both vascular and total extravascular accumulation of albumin in various tissues in control and ANP-treated rats. This approach has many advantages over single tracer methods. First, by accounting for tracer accumulation in the vascular space of a tissue sample, errors due to gain or loss of tracer from the vascular space alone are reduced. Second, by taking into account the mean vascular tracer concentration over the period of tracer accumulation, the extravascular accumulation can be expressed as a plasma clearance of tracer. For the purpose of evaluating ANP's role in regulating vascular volume, we will show that the tissue-specific blood-to-tissue clearance (a measure of the plasma equivalent volume that is cleared from the circulation during a specific time period) can be directly compared with the renal excretion of water to concentrate the plasma proteins. Third, these clearance values provide a basis for further analysis of the mechanisms whereby ANP increases blood-to-tissue exchange. Specifically, an increase in clearance may be due to increased permeability, increased surface area for exchange (Sarelius & Huxley, 1990), increased entrainment of macromolecules with filtered fluid (solvent drag) (McKay & Huxley, 1995) or some combination of all the above.

Although the advantages of the two-tracer methods to investigate transvascular macromolecule exchange are becoming more widely recognized (for review see Nagy *et al.* 2008), their use with transgenic mouse models has been limited. Thus, a second aim of the present experiments was to adapt to mice the two-tracer isotope methods to measure albumin clearance, similar to those used by Renkin and colleagues, and to use these methods in both wild type mice and in mice with an endothelial targeted deletion of the ANP receptor as used by Sabrane and colleagues (Tucker *et al.* 1992; Sabrane *et al.* 2005). Also, while most of the effort in the present study was directed towards albumin clearances, the use of a smaller macromolecule, the gadolinium-based magnetic resonance (MR) contrast agent Gadomer with a molecular mass of 35 kD was also investigated. This second tracer not only provided an independent estimate of vascular permeability, but also enabled repeated measurements of vascular permeability within each mouse before and during ANP administration because it was rapidly cleared from the plasma by the kidney. A third aim of the studies was to evaluate an alternate method to measure microvessel permeability to macromolecules in mice using dynamic contrast-enhanced MR imaging (DCE-MRI) with the aim of enabling repeated measures of blood-to-tissue exchange in each mouse. The three aims required a strategy involving the collaboration between laboratories in Davis, Bergen and Würzburg. The two-tracer method which was used routinely in rat tissue in the Bergen laboratory (Nedrebo *et al.* 2003) and evaluated in detail in Davis (Tucker *et al.* 1992; Renkin & Tucker, 1996, 1998) was first modified and tested in wild type C57BL6 mice. Similarly, the MR imaging (MRI) using Gadomer which was being used to measure vessel permeability of contrast agents in rat brain tumours in Bergen (Nedrebo *et al.* 2003; Brekke *et al.* 2006) was tested to enable measurements in the wild type mouse masseter muscle and overlying skin. After modifying and testing these methods with the wild type mice, experiments were designed in collaboration with the Würzburg laboratory

using the EC GC-A KO mice and their control littermates to use the two-tracer approach and the MRI methods.

The initial focus was on ANP-regulated exchange in skeletal muscle and skin because these tissues along with the GI tract were most responsive to ANP in previous experiments in rat tissue (Tucker *et al.* 1992). Also, as noted above, skeletal muscle was one of the tissues in control awake mice where Sabine and colleagues measured increased albumin uptake (Sabrane *et al.* 2005). Further, as skeletal muscle represented up to 45% of body weight, as compared to GI tissues of approximately 3% body weight, it was expected that the interstitial space in skeletal muscle tissue was potentially the largest reversible sink for plasma protein and fluid exchange from blood to tissue. The results described below provide the first data from mice to indicate that, while ANP-modulated increases in vascular permeability of muscle and skin contribute to regulation, they are not sufficient to account for ANP modulation of plasma volume in the mouse models. Thus, one outcome of the present studies is the need to further develop both the two-tracer and MRI methods for applications in mice to evaluate ANP-dependent regulation of both permeability and exchange surface in tissues with high baseline permeability and capacity to exchange fluid such as the GI tract.

Methods

Animals

Female C57BL6 mice (body weight (BW) 25–30 g) were used for MRI experiments and the two-tracer clearance method. Also, to further explore the role of ANP in vascular permeability, female mice with endothelium-restricted deletion of the guanylyl cyclase A receptor gene (GC-A gene; floxed GC-A × Tie2 Cre: EC GC-A KO) and their control littermates (floxed GC-A, with normal GC-A expression levels) were included in the study (BW 23–40 g). These mice are of a mixed genetic background (129Sv × C57BL6). Details of these mice have been previously published (Sabrane *et al.* 2005). The same mice were used for both MRI and the two-tracer method. The mice recovered fully from the MRI experiments and were used for the two-tracer clearance measurements after 2–3 days. All animals were anaesthetized with 3.5% isoflurane (Isoba vet, Schering-Plough Animal Health) and maintained with 1.5–2% isoflurane (Isoba vet), in air supplied via a nose cone. Mice used only for MRI scanning were not killed and were returned to the animal house. The mice were monitored continuously for respiratory rate and temperature. Blood pressure was not monitored as only a single tail vein catheter was used for fluid infusions. In previous experiments using conscious mice (floxed controls) Dr Kuhn and colleagues measured a slight fall in mean arterial pressure in mice with the same genetic background from 85 ± 3 (106/75) mmHg to 80 ± 2 (97/70) mmHg after 25 min of ANP infusion (Lopez *et al.* 1997). As shown below, there was no significant change in local intravascular volume in EC GC-A KO mice *versus* their control littermates in the presence of ANP. Mice were killed with saturated KCl at the end of the tracer accumulation for tissue collection (see below). All animal procedures were performed in accordance with protocols approved by The National Animal Research Authority (Oslo, Norway) and comply with UK policies and regulations (Drummond, 2009).

ANP infusion

ANP (rat, synthetic, from Sigma-Aldrich) was dissolved in phosphate-buffered saline without potassium and infused via the tail vein at a dose of 500 ng (kg BW)$^{-1}$ min^{-1} using an infusion pump. This dose was previously used in mice (Sabrane *et al.* 2005) and was close to the dose used in comparable experiments in rats (400 ng (kg BW)$^{-1}$ min^{-1}) (Tucker *et al.* 1992).

Two-tracer clearance methods

As unbound radioactive iodine will compromise all measurements of tissue uptake of albumin, great care was taken to ensure that the amount of free iodine in the injectate was negligible. Human serum albumin (HSA) was labelled with ^{131}I by the Iodogen method and unincorporated ^{131}I removed by spinning the stock solution twice on a 3 kDa spinning column (Microcon filter; Millipore, Bedford, MA, USA). ^{125}I-HSA was purchased from the Institute for Energy Technology, Kjeller, Norway. The integrity of labelled HSA was verified by anionic exchange chromatography and high resolution size exclusion chromatography, using an online gamma detector in series with the UV detector. The elution pattern of iodinated HSA was not different from that of native HAS, and low molecular weight radioactivity accounted for less than 0.3% of the total activity.

^{125}I-human serum albumin (HSA) (0.05 MBq) in 0.05 ml of saline was given I.V. over 30 s and it circulated for 30 min before ^{131}I-HSA (0.05 MBq) in 0.05 ml of saline was given over 30 s. Five minutes after injection of ^{131}I-HSA, blood samples were obtained, and the mice were killed by an intracardiac injection of saturated KCl. Thereafter, tissue samples for evaluating blood-to-tissue clearance were obtained from skin of the back, skin of the tail, hamstring muscle, quadriceps muscle and from the trachea. The plasma and tissue samples were put in pre-weighed open vials, sealed immediately, and reweighed as soon as possible. After counting, the tissue samples were placed in a drying chamber at 60°C. The vials were weighed repeatedly until stable weight was measured

(usually after 2–3 weeks). The radioactivity in tissue and plasma samples was determined in a gamma-counting system (LKB Wallac 1285, Turku, Finland). Background activity and spillover from ^{131}I to ^{125}I were corrected automatically. Clearance was estimated as the extravascular plasma equivalent volume of ^{125}I-HSA (counts min^{-1} (g dry tissue weight)$^{-1}$/counts min^{-1} (ml plasma)$^{-1}$). This was calculated as the difference between the plasma equivalent distribution volume of ^{125}I-HSA at 35 min and that of ^{131}I-HSA at 5 min, i.e. as a clearance over 30 min. All calculations were referenced to tissue blood-free dry weight as previously published (Nedrebo *et al.* 2003).

MRI

We evaluated the use of MRI to measure blood-to-tissue clearances of Gadomer (kindly provided by Bayer Schering Pharma, Germany), a gadolinium-based MR contrast agent with an apparent molecular mass of 35 kD (Misselwitz *et al.* 2001) as a comparison to vessel permeability of radio-labelled albumin. DCE-MRI (T1-weighted FLASH sequence with repetition time (T_R) and echo time (T_E) of 11.1 and 2.5 ms, respectively, and a flip angle of 25 deg) was performed using a small animal horizontal bore 7T Pharmascan (Bruker Biospin MRI, Ettlingen, Germany) and a dedicated mouse bed and mouse head coil. Images were acquired with a slice thickness of 1 mm and a temporal resolution of 0.795 s. Total number of imaging frames was 500. The contrast agent (0.1 mmol (kg BW)$^{-1}$, in saline) was injected through the tail vein after acquisition of 30 baseline images. Each animal served as its own control as identical imaging protocols were conducted before and after ANP infusion (1 h between each Gadomer injection). The mice fully recovered from MRI measurement and were subsequently used for the double-tracer experiments. Mice used only for MRI scanning were not killed and were returned to the animal house.

The signal intensity over time was followed in selected regions of interest (ROIs) in the masseter muscle and head skin. Signal intensity in blood vessels was also measured in small ROIs placed over maxillary, alveolaris and facial arteries and converted to tracer concentration over time assuming a linear relationship between signal intensity change and tracer concentration. Controlled injection for 10–12 s caused an initial 'step' increase in signal intensity as the vascular volume was filled. Subsequent blood-to-tissue tracer exchange resulted in further (initially linear) increases (slope) in tracer intensity over periods of 100–300 s. Apparent solute permeability coefficients (P_s) to Gadomer in tissue ROIs free of major vessels was calculated from the slope and step, assuming a microvessel volume to surface ratio of 4.4 μm (details in Results) (Curry *et al.* 1983). Corrections for the fall in plasma concentration (Gadomer cleared from plasma within 1 h) increased estimates of P_s by 10–20%. This correction was based on a simple compartmental model that took into account tracer exchange into the interstitium as well as the fall in plasma concentration over the initial 10–15 min of Gadomer exchange. The same model applied to albumin accumulation over 30 min (longer time, less permeable molecule, and slower fall in plasma concentrations) indicated errors of close to 10%.

Results

Figure 1*A* shows measurements of the action of ANP to increase extravascular albumin tracer accumulation in mouse tissue using the two-isotope tracer method in C57BL6 mice. Tracer accumulation was measured as an equivalent volume of plasma (clearance) with units of μl (g dry wt)$^{-1}$. The 30 min albumin clearances with vehicle (saline) controls ($n = 16$ mice) were 7.9 ± 1.6 and 19.7 ± 4.1 in tail and back skin, respectively, and 6.5 ± 1.6 and 10.6 ± 1.9 in hamstring and quadriceps muscle, respectively. There was a statistically significant increase in the extravascular albumin accumulation with ANP infusion, compared to vehicle control in tail skin (15.5 ± 1.6, $P = 0.005$; a 1.96-fold increase); back skin (33.8 ± 2.3, $P = 0.027$; 1.7-fold increase) and hamstring muscle (12.7 ± 1.6, $P = 0.013$; 1.95-fold increase) (all $n = 16$). The increase in quadriceps muscle (12.0 ± 0.8, $P = 0.55$; 1.2-fold) and trachea which had a high base line accumulation (86 ± 19.6 *vs.* 40 ± 3.7; $P = 0.13$; 2.2-fold) were not statistically significant.

Figure 1*A* and *B* together show that the vehicle control intravascular volumes (albumin reference tracer) were larger than 30 min albumin tissue clearances in skin and muscle. For example, in muscle, 30 min albumin clearance was as small as 6.5 ± 1.6 μl g^{-1} and intravascular volume was 20.1 ± 2.6 μl g^{-1}. In back skin, 30 min clearance was 19.7 ± 4.1 μl g^{-1} and intravascular volume was 21.7 ± 2.3 μl g^{-1}. As 30 min albumin clearances were calculated as the difference between plasma equivalent volumes measured at 35 min with albumin-I^{125} (total vascular and extravascular accumulation) and at 5 min with albumin-I^{131} (intravascular tracer distribution; the measure of intravascular volume in each tissue sample), changes in vascular volume may be an important variable affecting estimates of tissue clearance. There was no statistically significant trend for mean values of intravascular volume to increase with ANP, but there was a tendency to increase intravascular volume in tail skin and trachea. Furthermore, there was also a tendency for individual estimates of clearance to be higher when the measured intravascular volume was also higher, suggesting that a simple correction for the amount of tracer in the

intravascular volume may not be sufficient to correct for changes in intravascular volume. This trend was noted in tail skin and trachea but not in muscle, and suggested the need for additional evaluation of factors such as an increase in surface area for exchange secondary to a small increase intravascular volume as discussed below. These observations emphasize the importance of accurate measurement of changes in intravascular volume when estimating extravascular tissue accumulation over 30 min. We addressed this problem further as follows.

Figure 2 shows the result of normalizing the 30 min tissue clearances by dividing each measured value (volume (g dry wt)$^{-1}$) by intravascular volume (also in volume (g dry wt)$^{-1}$). If the increase in tissue accumulation with ANP reflected only an increase in surface area, proportional to the number of perfused microvessels and local intravascular volume, the normalized tissue clearance values in the presence of ANP would not be significantly increased. The statistically significant increase in the normalized clearance in back skin ($P = 0.023$), tail skin ($P = 0.016$) and hamstring muscle ($P = 0.034$) supports the hypothesis that the increase in tissue accumulation by ANP in these tissues is predominately due to a change in the mechanisms of blood-to-tissue exchange (by increased diffusive and/or convective transport) and not just a change in overall surface area due, for example, to vasodilatation. Even though intravascular volume tended to increase in trachea, there is still an increase in normalized clearance in the trachea, suggesting that the increase in albumin clearance in the trachea may not be due only to increased surface area for exchange.

We next used the two-tracer isotope method to measure ANP-dependent increases in albumin clearance in mice with endothelial-restricted deletion of the guanylyl cyclase-A (GC-A) receptor for ANP (EC GC-A KO) and their control littermates. There was a significant increase in albumin clearance in back and tail skin, and hamstring muscle of control littermate mice exposed to ANP relative to vehicle treatment but no significant increase in albumin clearance in muscle or skin tissue of the KO mice when exposed to ANP relative to vehicle treatment. A comparison in KO mice without (open bars) and with ANP (clear hatched bars) is shown in Fig. 3 as normalized ratios for contrast with the ANP-dependent increase in the control littermates without (filled bars) and with ANP (filled hatched bars). The increase in normalized clearance in control mice ($n = 6$) was significant when measured relative to the vehicle (no ANP; *; $n = 5$), or the ANP-treated KO mice (**; $n = 5$). For example, in back skin the normalized clearance increased from 0.67 ± 0.07 to 1.36 ± 0.31 ($P = 0.02$), in tail skin from 0.46 ± 0.03 to 1.02 ± 0.54 ($P = 0.003$), and in hamstring muscle from 0.33 ± 0.05 to 0.42 ± 0.07 ($n = 6$; $P = 0.048$). There were similar results in muscle tissue in the tongue (data not shown). The absolute values of the 30 min clearance values in muscle of both the control littermates and the KO mice in the absence of ANP were similar. For example, in the control littermates the 30 min albumin clearances were 3.5 ± 0.5 and $3.9 \pm 0.6\ \mu l\ g^{-1}$ in quadriceps and

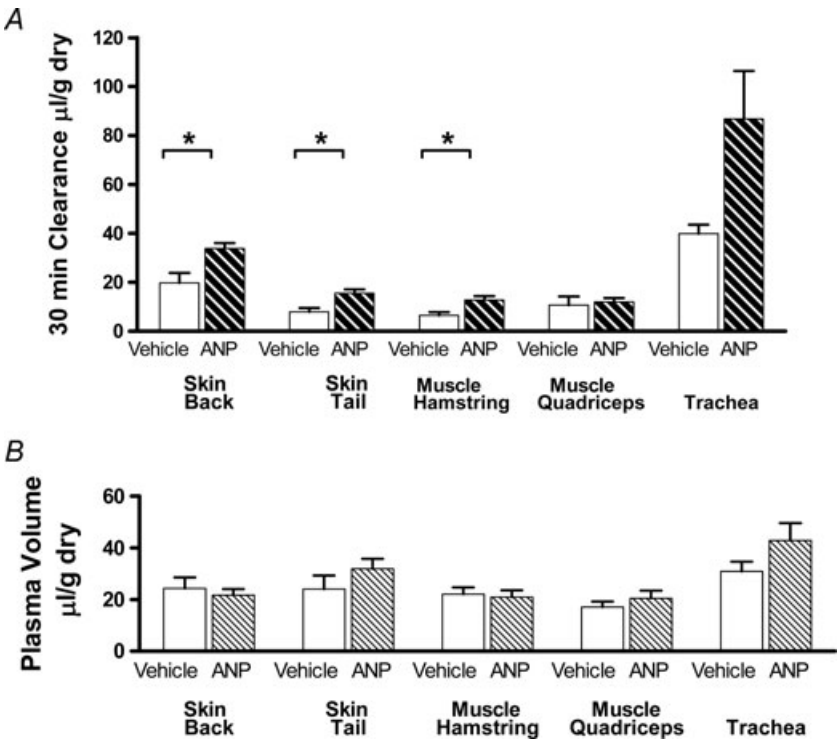

Figure 1. Albumin clearance and plasma volume measured in C57BL6 mice with and without ANP
A, the clearance of albumin in skin, muscle and trachea in wild type C57BL6 mice with no ANP (control; open bars) and C57BL6 mice with continuous infusion of ANP (0.5 ng min^{-1} (g body weight)$^{-1}$; heavy hatched bars). The 30 min clearances were measured as the difference between the plasma equivalent volume containing the amount of albumin labelled with ^{125}I in the tissue (vascular plus extravascular space) after 35 min and the plasma equivalent volume of albumin labelled with ^{131}I measured after 5 min (mainly vascular space, and also used as a measure of tissue plasma volume. *B*, the figure shows that the amount of albumin in the extravascular space after 30 min may be less than or equal to the amount of tracer in vascular space. There was a tendency for ANP to increase albumin clearances in all tissues but only back and tail skin and hamstring muscle showed significant increases (*$P < 0.05$) relative to vehicle control. There was no significant effect of ANP on measured plasma volumes (light hatched bars in *B*). All values are expressed per gram of tissue dry weight.

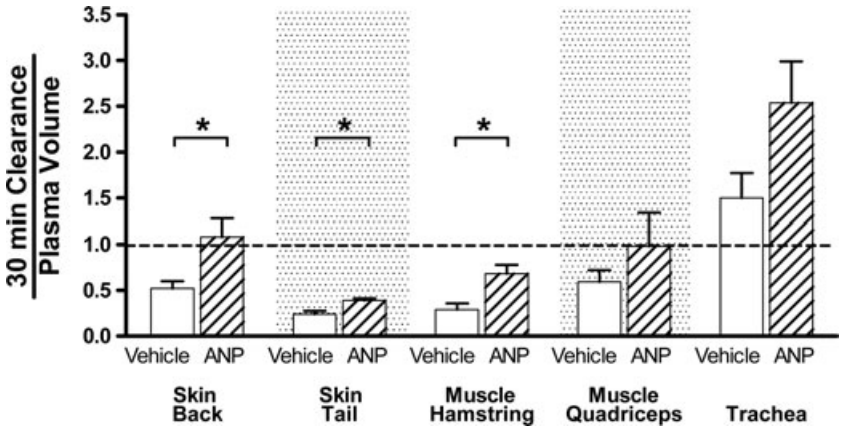

Figure 2. Clearances (30 min) in wild type C57BL6 mice with (hatched bars) and without ANP (open bars) were normalized to the measured plasma volume in each tissue (data from Fig. 1)
The normalization reduces some of the variability in the data (*$P < 0.05$). Furthermore, the significant increases in the normalized clearance (in back and tail skin and hamstring muscle) are consistent with a real increase in vascular permeability, not just an increase in surface area for exchange. The alternating background stipple separates different tissue samples. Normalized clearances falling below the broken line indicate 30 min clearances smaller than the measured plasma volume in the tissue sample. Note that the units of the 30 min clearance are μl (g dry weight)$^{-1}$. Thus, a 30 min clearance is a real clearance (expressed as a rate (ml g^{-1} min^{-1}) multiplied by a measuring time (min).

hamstring muscles, respectively, and in back skin the 30 min clearance was $4.7 \pm 1.0\ \mu l\, g^{-1}$. In the KO mice, the corresponding quadriceps and hamstring values were 3.0 ± 0.9 and $3.6 \pm 0.5\ \mu l\, g^{-1}$ and in back skin the control littermate 30 min clearance was $5.2 \pm 0.6\ \mu l\, g^{-1}$. These absolute values, and the magnitude of the normalized clearance increases shown in Fig. 3 (less than 1.5-fold in muscle and less than 2.2-fold in skin), are important for the purpose of evaluating the contribution of ANP-dependent changes in microvascular endothelial permeability of muscle and skin to the overall modulation of plasma volume (see Discussion).

A limitation of all the experiments described above is that each mouse can be studied at only a single point of time, and different mice must be used for vehicle and ANP studies. Figure 4*A* is an MR image of the mouse

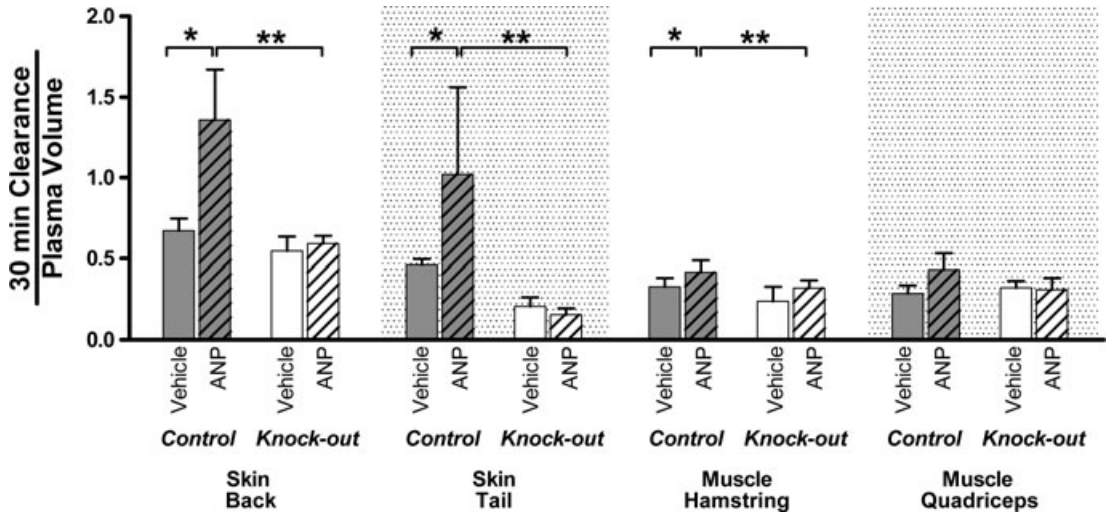

Figure 3. Comparison of the action of ANP (hatched bars) to increase albumin clearance in mice with endothelial-specific KO of the ANP GC-A receptor (open bars) and their control littermates (dark bars)
The format is the same as used in Fig. 2 for the wild type mice. In KO mice, ANP does not significantly increase normalized albumin clearance relative to vehicle controls. On the other hand, normalized albumin clearance in the presence of ANP is significantly increased in control littermates relative to the vehicle control (*) and relative to ANP-treated KO mice for back skin, tail and hamstring muscle (**). Note that the units of the 30 min clearance are μl (g dry weight)$^{-1}$. Thus, a 30 min clearance is a real clearance (expressed as a rate (ml g^{-1} min^{-1}) multiplied by a measuring time (min).

head, showing Gadomer uptake and typical ROIs in an artery, masseter muscle and skin tissue of a C57BL6 mouse 200 s after injection of the contrast agent into the tail vein. Figure 4*B* visualizes the change in signal intensity due to tracer uptake in various tissues (i.e. a subtraction image generated by subtracting a baseline image from the image in Fig. 4*A*). Measurements were first made in C57BL6 mice to establish the conditions where reliable measurements

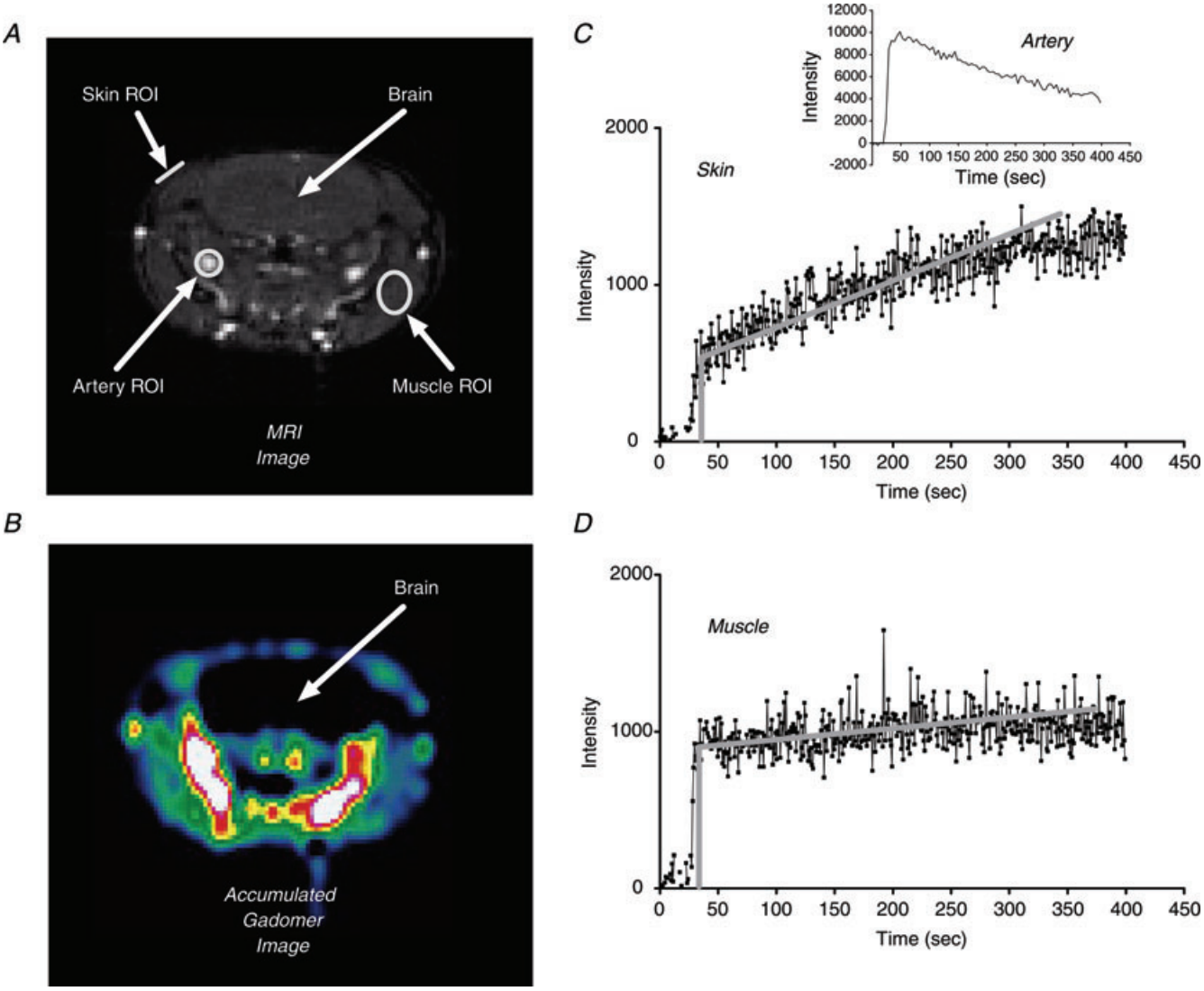

Figure 4. Measurement of 35 kD Gadomer contrast agent apparent permeability coefficient in skin and muscle tissue of C57BL6 control mouse muscle and cheek during vehicle (saline) infusion
A, MR image (axial slice) of mouse head acquired 200 s after contrast agent injection via the tail vein. The ROIs were carefully selected using anatomical references for muscle, skin and vessels. *B*, shown is the subtracted image (image in *A* minus baseline image) recording the signal increase in tissue after injection of Gadomer, where cold colours indicate low signal enhancement and warm colours indicate high signal enhancement. Note the high signal intensity in large arteries showing that most of the high molecular weight Gadomer contrast agent is mainly in the vascular space. *C*, curve showing the signal intensity changes over time in a ROI used to estimate Gadomer permeability coefficient in the skin. As the contrast agent is injected there is a step increase in tracer signal intensity above background as the vascular volume in the ROI is filled with the contrast agent. Tracer continues to accumulate in the ROI as it enters the extravascular space. The initial rate of tracer accumulation is estimated from the slope of the signal intensity over the first 100–150 s. An initial estimate of the vascular permeability is obtained from the magnitude of the initial slope and step. This initial estimate can be corrected for the fall in vascular tracer concentration (as measured from the signal intensity over an adjacent artery; see inset). *D*, signal intensity over time in ROI over masseter muscle. Muscle permeability is less than in skin. The analysis to estimate vascular permeability is over an ROI containing no vessels larger than 100 μm diameter. Thus, assuming a mean plasma volume to exchange surface area of 4.4×10^{-4} cm, the vascular permeability coefficients in muscle and skin tissue were $4.6 \pm 0.6 \times 10^{-7}$ cm s^{-1} and $26 \pm 3 \times 10^{-7}$ cm s^{-1}, respectively.

could be made in muscle and skin tissue. The mouse head was chosen for these measurements because it had the least amount of tissue movement and the same region of muscle and skin tissue could be imaged first with a vehicle alone, then after infusion of ANP. The P_s to Gadomer in tissue ROIs free of major vessels was calculated from the rate of increase in contrast agent accumulation (slope of the signal intensity) after filling the vasculature (initial step; see Fig. 4). The ratio of the slope/step is equivalent to the normalized clearance ratios in Fig. 3 divided by the time of tracer accumulation. As shown in Appendix 2 this ratio can be expressed as an apparent P_s by multiplying the slope/step values by an estimate of the exchange area per intravascular volume in the tissue sample. As we avoided all vessels larger than 60 μm diameter in our selection of a ROI, we estimated a mean value of the local vascular volume to vascular surface area ratio (equal to radius/2) for cylindrical microvessels of 4.4×10^{-4} cm for the microvascular bed. This estimate was based on the assumption that half the surface area for exchange was in venular microvessels with a mean diameter of 30 μm and the other half in true capillaries with 5 μm diameter. Average Gadomer P_s values with vehicle infusion in C57BL6 mice were $4.6 \pm 0.6 \times 10^{-7}$ cm s^{-1} ($n = 12$; masseter muscle of the cheek) and $26 \pm 3 \times 10^{-7}$ cm s^{-1} ($n = 14$; adjacent skin of the mouse cheek). As shown in Fig. 4, Gadomer is cleared from the plasma much more quickly than albumin. Corrections for the fall in plasma concentration increase the permeability estimates in skin by 10–20%. ANP was then infused and the MRI experiment was repeated. Mean P_s in muscle ($6.7 \pm 0.9 \times 10^{-7}$ cm s^{-1}; $n = 10$) increased significantly in the presence of ANP relative to vehicle control ($P = 0.047$; 1.45-fold increase) and in skin to $49 \pm 7 \times 10^{-7}$ cm s^{-1} ($n = 12$; $P = 0.01$; 1.9-fold increase).

Measurements were then made on EC GC-A KO mice and their control littermates (Fig. 5). The mean Gadomer contrast agent apparent permeability coefficients in masseter muscle and skin in control littermate mice prior to ANP (vehicle) were $2.8 \pm 0.5 \times 10^{-7}$ cm s^{-1} ($n = 12$) and $16.8 \pm 1.5 \times 10^{-7}$ cm s^{-1} ($n = 10$). ANP increased the apparent permeability coefficient of both muscle (1.2-fold) and skin (1.45-fold), but the change in muscle tissue was too small to reach significance. Mean P_s increased to $3.4 \pm 0.5 \times 10^{-7}$ cm s^{-1} ($n = 18$; $P = 0.44$) in muscle of control littermate mice and to $24.5 \pm 2.0 \times 10^{-7}$ cm s^{-1} ($n = 12$; $P = 0.01$) in skin. In the KO mice the vehicle control permeability values were similar to the littermate controls but there was no significant increase in permeability. In fact, there was a tendency for the P_s values to be smaller than the vehicle controls. A unique feature of our experimental design was that the same mice were used in both the MR imaging experiments and the two-tracer isotope experiments. On each mouse we have paired measurements of Gadomer P_s with and without ANP, as well as one estimate of albumin clearance. As expected, the P_s estimates for the smaller macromolecule used as a contrast agent in the MR imaging experiments are larger than the values for albumin (estimates for albumin P_s in Discussion). However, the MRI experiments demonstrate that the same mouse can be used for additional measurements (e.g. longitudinal measurements with multiple MRI scans or a terminal two-tracer isotope clearance measurement to evaluate clearance in organs where MRI measurements may require calibration against a more well-established standard).

Discussion

Our results provide new direct measurements of blood-to-tissue exchange of albumin in both wild type and endothelial ANP receptor KO mice and their control littermates, which enable further evaluation of the role of ANP as a modulator of vascular volume by selective increase in tissue vascular permeability. First, quantitative measurements of blood-to-tissue exchange measured as either a normalized clearance (albumin) by the two-tracer method (Fig. 3) or an apparent solute permeability coefficient (Gadomer contrast agent) by MR imaging (Fig. 5) provide independent evidence that ANP increases blood-to-tissue exchange in skin and muscle of mice with

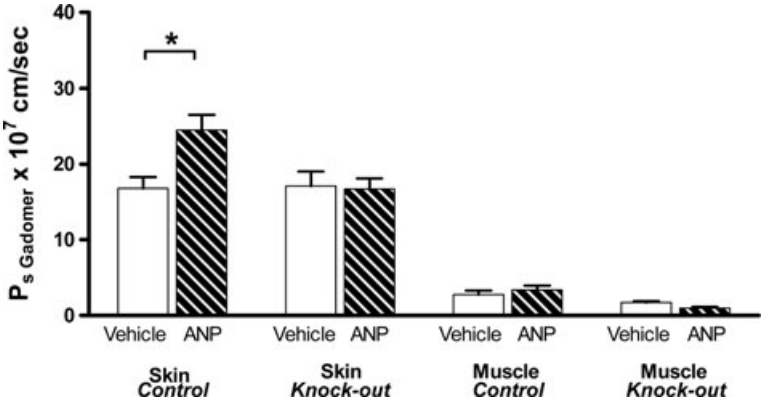

Figure 5. Mean values of 35 kD Gadomer contrast agent apparent permeability coefficients in masseter muscle tissue and skin of control and EC GC-A KO mice before (open bars) and after (hatched bars) infusion of ANP
Using the slope/step method in Fig. 4, paired measurements of Gadomer tracer permeability were made before and after ANP infusion in mice later used for the two-tracer isotope uptake methods summarized in Fig. 3. ANP increased cheek skin permeability coefficient (*$P < 0.05$) and there was a small increase in muscle. In the presence of ANP there was no significant permeability increase in skin or muscle of EC GC-A KO mice.

normal endothelial GC-A receptors for ANP, and fails to do so in mice with endothelial-restricted deletion of the GC-A receptor for ANP. These results conform to the hypothesis that ANP regulation of vascular permeability is critically involved in plasma volume regulation because Sabrane and colleagues showed that the acute ANP-induced reduction in vascular volume is abolished in EC GC-A KO mice even though renal water excretion in these mice is normal (Sabrane *et al.* 2005). Second, the major new contribution to understanding this ANP-dependent mechanism is that quantitative measurements of albumin clearance enable determination of the contribution of ANP-dependent permeability changes in specific microvascular beds to plasma volume regulation. We discuss skeletal muscle and skin below.

First we will evaluate the methods. Figure 1 clearly demonstrates that small increases in vascular volume may introduce significant errors in the estimate of real extravascular tracer unless the vascular volume is actually measured in each experiment. As is becoming more widely recognized, the problem is particularly acute when only one tracer is used as there is no independent measure of vascular volume (Nagy *et al.* 2008). We note, however, that even though the use of two-tracer methods to account for changes in both vascular and extravascular tracer accumulation provides more reliable measures of blood-to-tissue exchange, the method has limitations that must be taken into account when interpreting the mechanisms whereby ANP modulates macromolecule exchange. While the two-tracer method accounts for tracer accumulation in the vascular volume, increased local tissue perfusion may also increase the surface area for exchange, leading to increased tracer accumulation without increased permeability of the transvascular pathways. Thus, an increase in clearance is not necessarily due to increased permeability alone. A new aspect of the two-tracer analysis introduced in Fig. 2 is normalization of the 30 min clearance by the measured vascular volume. The advantage of using the ratio between clearance and plasma volume is that each experiment is treated individually. Assuming that the added plasma volume is new vascular tissue with the same properties as before, i.e. microvessels with the same distribution of diameters, this is a correct estimate of the changes in surface area induced by ANP. However, if the additional plasma volume involves increased mean diameter of the exchange vessels, the correction for changes in surface area would be less and the approach would underestimate the real increase in permeability. We emphasize that 70–80% of the vascular volume is outside the microvasculature. The normalization is applied using only the local intravascular volume in the same sample as the tracer accumulation is measured. Also, even though there is some loss of the vascular tracer during a 5 min measuring period for this second tracer, the error in estimating 30 min clearances is expected to be small because an equivalent amount of the first tracer would be lost in the first 5 min of circulation. The 30 min clearance is measured as the difference in tissue tracer accumulation between 5 and 35 min.

In both C57BL6 mice and control littermates of EC GC-A KO mice, normalized clearances in muscle and skin in the presence of ANP infusion were significantly increased. This result is consistent with a true increase in permeability, but it does not eliminate the possibility that increased tissue accumulation of albumin is the result of increased solvent drag (i.e. coupling of albumin flux to any transvascular water flow; see Appendix 2 for details) or of increased solvent drag in addition to increased permeability. We do not distinguish between diffusion and solvent drag when referring to clearance measurements in these experiments, but we do make preliminary estimates of the contribution of solvent drag to net blood-to-tissue exchange in the section below. Tucker and Renkin found that raising microvascular pressure by applying a tourniquet to one leg after exposure to ANP did not significantly increase tissue solute accumulation relative to the leg with normal pressure, suggesting that solvent drag does not contribute significantly to increased solute flux in muscle or skin (Tucker *et al.* 1992). We also note that in the C57BL6 mice, ANP tended to increase local vascular volume in trachea as well as increase extravascular accumulation. If there was a significantly increased area for exchange proportional to vascular volume then the normalized clearance in trachea would not have increased. That normalized clearance increased close to 1.5-fold in trachea of C57BL6 mice suggests that increased permeability contributed at least partially to the increased clearance in the trachea. In summary, the analysis based on normalized clearance conforms to the hypothesis that the primary mechanism to increase albumin clearance in these experiments was a real increase in vascular permeability.

As shown in Appendix 2, the normalized clearances in Fig. 2 can be expressed as an apparent albumin permeability coefficient. To do this, values in Fig. 2 were divided by the time of albumin accumulation for clearance measurements (30 min) and then multiplied by an estimate of the exchange area per unit intravascular volume in the tissue sample. If we use the same microvascular volume/surface area ratio as for the permeability estimates based on MRI data (4.4×10^{-4} cm), the control normalized clearances in Fig. 2 correspond to apparent permeability coefficients for albumin ranging from 0.8×10^{-7} cm s^{-1} in hamstring muscle, to 1.5×10^{-7} cm s^{-1} in skin, and up to 3.5×10^{-7} cm s^{-1} in trachea. These values would be doubled if all the transvascular exchange of albumin was in venular capillaries, and would be reduced by about 40% if all the exchange occurred through the smaller vessels (true capillaries with diameter of 5 μm).

The uncertainties in using this estimate of microvascular volume/surface are larger in the two-tracer method where larger vessels may contribute to the measured local intravascular volume. These values appear reasonable because the measured permeability coefficients in muscle for the smaller Gadomer tracer (35 kD *vs.* 65 kD albumin tracers) are close to 5 times larger than that of albumin in skin and muscle of the same mice as the isotope measurements were made. Furthermore, measurements of apparent albumin permeability coefficients from permeability–surface area product (PS) values in mammalian hind limb skeletal muscle also fall below 1×10^{-7} cm s^{-1} (Michel & Curry, 1999) although higher values are also reported (e.g. 9.9×10^{-7} cm s^{-1} in arterioles and 44×10^{-7} cm s^{-1} in venular vessels of mouse cremaster muscle (Sarelius *et al.* 2006)).

We also note that our absolute values of tissue clearance in muscle and skin in mouse tissue are similar to values measured in rat. For example, Tucker and colleagues measured baseline albumin clearances in rat muscle tissue (tibialis anterior and lateral gastrocnemius as 0.15 ± 0.1 and 0.17 ± 0.1 μl min^{-1} g^{-1}, respectively) (Tucker *et al.* 1992). Expressed in the same units, vehicle control albumin clearances in C57BL6 mice were 0.22 ± 0.04 and 0.35 ± 0.07 μl min^{-1} g^{-1} in mouse hamstring and quadriceps muscle and were 0.11 ± 0.03 μl min^{-1} g^{-1} in the muscle of KO mice. Values for skin in rat were (μl min^{-1} g^{-1}): 0.24 (leg skin) and 0.28 (back skin) compared with 0.65 (back skin) and 0.26 (tail skin) in C57BL6 mice. ANP increased clearance in muscle tissue of rat by 1.5- to 1.6-fold and 1.2- to1.3-fold in skin (Tucker *et al.* 1992).

We conclude that the two-tracer method as applied to mouse tissue provides a reliable measurement of blood-to-tissue clearance of macromolecules such as albumin in mice. Further, the clearance/plasma volume ratio is a useful index to distinguish changes in apparent permeability (diffusion with possible contributions from solvent drag) and changes in surface area for exchange. This approach has the potential to provide a common standard for comparisons between investigations involving the use of transgenic mice and their control littermates in investigations of the regulation of vascular permeability. Its limitation is that mice are killed to obtain tissue samples so that control and test samples require different mice and longitudinal studies on the same mouse are not possible. To this end, the experiments using the contrast agents with higher molecular masses such as Gadomer provide an important new approach in mouse studies. With its intermediate molecular mass, this tracer is more permeable than albumin in the vascular wall and has permeability properties similar to tracers such as α-lactalbumin, a tracer used in our laboratory to measure changes in the vessel permeability in isolated perfused mesenteric microvessels (Huxley *et al.* 1987). An advantage of this is the relatively rapid removal from the plasma by renal filtration allowing repeated measurements on the same animal within 1 h. Loss of Gadomer from the plasma volume during tissue accumulation was found to lead to underestimates of skin permeability coefficients using the initial (slope/step) uptake analysis (Appendix 2) of the order of 10–15%. Preliminary estimates indicate that a larger underestimate may result (up to 50%) when permeability coefficients are smaller, as in muscle tissue (less rapid tracer accumulation). These limitations do not compromise the main results reported above that the fractional increases in muscle and skin permeability of C57BL6 and control littermates for Gadomer in response to ANP were similar, and that Gadomer permeabilities were not increased in response to ANP in the EC GC-A KO mice. Further measurements using Gadomer were carried out on the same EC GC-A KO mice and their littermates as used for the two-tracer measurements showing the potential for longitudinal studies.

Control of vascular volume

To understand the role of ANP in the regulation of vascular volume it is important to distinguish the action of a diuretic such as furosemide from the action of ANP in the regulation of extracellular fluid volume. Trippodo and Barbee demonstrated that the extracellular fluid excreted by the kidney in response to furosemide comes mainly from the interstitial space (Trippodo & Barbee, 1987). In contrast, more than half the fluid excreted by the kidney in response to ANP comes from the plasma space (Trippodo & Barbee, 1987; Renkin & Tucker, 1996). The reason for this difference is that fluid loss, initially from the vascular space during renal water excretion, concentrates the plasma proteins in the vascular space. With furosemide there is no increase in vascular permeability, and the elevated plasma protein oncotic pressure leads to exchanges in fluid from the interstitial space into the vascular space as the Starling forces governing transvascular fluid exchange shift towards net re-absorption as the plasma protein concentration increases. In this way, significant amounts of fluid can be excreted from the interstitial space by first being reabsorbed into the vascular space from the interstitium and then excreted. In contrast, ANP selectively increases vascular permeability at the same time the diuresis is occurring. There is a shift of the concentrated plasma protein from the vascular to the interstitial space, reduced rate of plasma protein concentration, reduced reabsorption from the extravascular space and preferential loss of fluid from the plasma space. Thus, for ANP to act mainly to regulate plasma volume, the rate of increase of plasma protein concentration in response to a urine flow during diuresis must not exceed the rate that plasma

protein concentration falls as a result of blood-to-tissue transport of the plasma protein due to increased vascular permeability (see derivation in Appendix).

It is also important to distinguish between changes in vascular permeability in the presence of increased renal water excretion and changes in vascular permeability to plasma proteins in the absence of increased water excretion. The most common example of the latter is an inflammatory state where the increase in plasma protein permeability results in plasma protein movement into the interstitium and an associated fluid shift as expected from the decreased plasma protein osmotic pressure difference. These inflammatory increases in permeability are generally larger than the more subtle increases measured in the present experiments with ANP (acute increases up to 5- to 10-fold for inflammatory mediators compared with 1.5- to 2-fold increases with ANP). Thus, at least in the acute state, the amounts of plasma protein exchanged into the interstitium with ANP are relatively small with ANP modulation. Furthermore, we will argue below that they are of a magnitude that can offset increases in plasma protein concentration due to water excretion by the kidney (a doubling of water excretion in the mouse would increase plasma protein concentration by 2 to 3% in the absence of increased permeability). We note, however, that in nephrectomised animals there is no mechanism to concentrate the plasma proteins (Almeida *et al.* 1986). We evaluate the contribution of increased blood-to-tissue exchange by ANP to the regulation of plasma volume by ANP below.

The simplest case to evaluate is when most of the blood-to-tissue exchange is due to a real increase in vascular permeability and any fluid shift from blood to tissue (for example through large unselective pores formed by ANP) is small. Taking albumin as representative, plasma albumin concentration will not significantly increase during an ANP-induced diuresis in a mouse with normal endothelial ANP receptors if the increase in urine flow rate is less than or equal to the increase in total clearance of albumin from blood to tissue. We evaluate this criterion using estimates of albumin clearance in skeletal muscle and skin as follows. Clearance of albumin in skeletal muscle during vehicle infusion in EC GC-A KO mice and their control littermates is 3.0–3.9 μl (30 min)$^{-1}$ (g dry weight)$^{-1}$. Assuming these values are representative of other skeletal muscles, mice with 40–45% body weight skeletal muscle (wet/dry weight close to 4; 75% water) are expected to have a mean baseline whole body albumin clearance from blood to tissue close to 0.78 μl h^{-1} (g body weight)$^{-1}$. The largest increase in skeletal muscle clearance in control littermate mice relative to EC GC-A KO mice in the presence of ANP was of the order of 1.5-fold (Fig. 3) in hamstring muscle. This would indicate a maximum estimate of clearance into skeletal muscle of 1.2 μl h^{-1} g^{-1}. This is larger than maximum whole body clearance (1.0 μl h^{-1} g^{-1}) estimated from the clearance of hamstring muscle in the presence of ANP in control littermates and is likely to place an upper limit on the contribution of increased skeletal muscle albumin clearance in the presence of ANP in these mice (1.2–0.78 = 0.4 μl h^{-1} g^{-1}). A similar set of calculations for skin (20% body weight) gives a baseline clearance of 0.47 μl h^{-1} g^{-1} and ANP-induced total body clearance of 1.1 μl h^{-1} g^{-1}, leading to an ANP-induced increase in clearance on a whole body basis of 0.6 μl h^{-1} g^{-1}. Thus, the combined increase in albumin clearance into skin and muscle is close to 1 μl h^{-1} g^{-1}.

We do not have estimates of the ANP-induced increase in water excretion in the EC GC-A KO or control littermate mice but the baseline urine flow in both groups was close to 1.3 μl h^{-1} g^{-1} (based on 30 μl day^{-1} g^{-1}) (Sabrane *et al.* 2005). A key observation is that the increase in albumin clearance into skin and muscle is of the same order of magnitude as baseline urine flows, so evaluation of contribution of skeletal muscle and skin to the overall vascular volume control depends heavily on the ANP action on renal water excretion under the conditions of these experiments. During ANP treatment urinary water loss in anaesthetised rats increased to 2 times control (Tucker *et al.* 1992) and to 4.3 times control (Trippodo & Barbee, 1987) in earlier measurements. Thus, if water excretion in the presence of ANP doubled in both EC GC-A KO mice and their control littermates (an increase of 1.3 μl h^{-1} g^{-1}) the combined albumin clearance in skin and muscle would account for close to 80% (1.0/1.3) of that required to meet the criterion of no net increase in plasma protein concentration and no net tendency for reabsorption. Loss of this function in the EC GC-A KO mice would account, at least in part, for the failure of these animals to control plasma volume. Furthermore, when this mechanism is intact in control animals, albumin clearance into skin and skeletal muscle enables maintenance of constant plasma volume in the face of urinary water loss. The surprising conclusion from the above calculations is that skeletal muscle with the largest total interstitial fluid volume accounts for a maximum of 30% of the albumin clearance needed.

Similar conclusions are drawn when the combined skin and muscle clearances in C57BL6 mice are analysed (data from Fig. 1) even though the baseline clearances are close to 2 times the values measured in the EC GC-A KO and control littermates. The increase in skeletal muscle clearance was 1.1 μl h^{-1} g^{-1} and the increase in skin clearance was 4.0 μl h^{-1} g^{-1}. In the C57BL6 mice using the methods of Kishimoto and colleagues (Kishimoto *et al.* 1996) the basal rate of water excretion measured during three 15 min intervals during a control vehicle saline infusion into female wild type mice under isoflurane anaesthesia was 1.38 $\pm$ 0.22 μl h^{-1} g^{-1} (M. Kuhn, unpublished observation). Water excretion

measured over three subsequent 15 min periods in the same mice during ANP infusion increased an average of 5.1 ± 0.8-fold (an average increase in water excretion expressed in units of μl h^{-1} (g body weight)$^{-1}$ of 5.6) under the conditions of their experiments. Thus, assuming a similar increase in water excretion, the combined skin and muscle increase in clearance (5.1 μl h^{-1} g^{-1}) is close to 90% of that required to regulate vascular volume. The skeletal muscle clearance on a whole body basis in the C57BL6 mice is 20% of that needed for skeletal muscle to be the dominant sink for plasma proteins. The fractional increase in permeability in mouse masseter muscle for the 35 kD Gadomer contrast agent (less than 1.2-fold) also demonstrates the relatively small response of skeletal muscle tissue to ANP. These results are consistent with the conclusions of Tucker and colleagues in rats exposed to a similar concentration of ANP that exchange of albumin into muscle interstitial space could not account for all albumin loss from the vascular space during exposure to ANP (Tucker *et al.* 1992). They estimated muscle accounted for less than 25% of the protein loss from the vascular space.

The analysis described above was based on the limiting case where there was no significant fluid loss into the interstitial space. If there is such fluid exchange, the plasma volume is decreased not only by renal water excretion but also by fluid loss into tissue. One possibility would be the loss of fluid containing the same protein concentration as in plasma as has been suggested to occur in the spleen (Hamza & Kaufman, 2009) or through large pores in a heterogeneous endothelial barrier containing large pores and small pores. For these large pores, the increased fluid flow would result from an increase in microvascular pressure, not a change in protein redistribution. The contribution of such fluid loss can be estimated from the mass balance in Appendix 1. This estimate is for the case where the solvent drag reflection coefficient in a large pore system is close to zero so the clearance of albumin via such pathways is equal to the actual fluid loss into the tissue and plasma protein content and water are lost from the vascular space in equal proportions (see Appendix 1). According to the above calculations based on a mass balance for plasma protein, this fluid loss would be between 10–20% of urine flow rate, as the combined clearance for skin and muscle accounted for 80–90% of urine flows. We note that the mass balance in Appendix 1 shows that for fluid shifts out of the vascular space to be larger than 10–20% of urine flow, the contribution of the other pathways (including the clearance estimates in skin and muscle) would have to be smaller than we have estimated. This would most probably be the result of heterogeneity in the response of muscle or skin tissues to ANP.

There are a number of topics for further evaluation with respect to ANP regulation of vascular permeability and volume. One is the assumption that the increase in skeletal muscle and skin albumin clearance induced by exogenous ANP relative to the increase in renal water excretion measured in these experiments is similar to that in acute or sustained increases in plasma volume leading to physiologically appropriate endogenous ANP release. There is support for this assumption for acute hypervolaemia in rats where the magnitude and distribution of albumin clearances measured during infusion of ANP at rates spanning that used in these experiments was similar to measured albumin clearance during acute plasma volume expansion. This is a topic for further study in mouse models of ANP-dependent volume regulation. Another issue is whether the 30 min clearances are characteristic of the mechanisms determining more long-term changes in protein distribution (for example, after the initial fluid movement there may be additional changes in the Starling forces determining fluid distribution including capillary and tissue pressures, and effective protein concentration in the interstitial space which depend on exclusion volumes and the lymphatic drainage of tissues). The contribution of tissues other than skeletal muscle also remains to be determined but there are useful clues from our own data and from previously published investigations. In control rat tissue, Tucker and Renkin measured albumin clearances in jejunum and colon that were 5 to 10 times larger than in skin and muscle on a dry weight basis (Tucker *et al.* 1992) and increased close to 2-fold with ANP (Renkin & Tucker, 1996). As noted above, Sabrane and colleagues reported that accumulation of albumin in colon, jejunum and duodenum was reduced by up to 50% of controls in the EC GC-A KO mice (Sabrane *et al.* 2005). If similar permeability properties apply in mice, a 2-fold increase in clearance in these GI tissues (2 to 3% body weight) could account for a net clearance of 0.5 to 1 μl h^{-1} (g body weight)$^{-1}$. However, a more detailed evaluation of the GI tissues as a contributor to the ANP-dependent regulation of vascular permeability and plasma volume is required. Also, the contribution of other compartments such as the extrasplenic microvasculature remains to be evaluated relative to the skeletal muscle and skin (Brookes & Kaufman, 2005; Hamza & Kaufman, 2009).

In summary, we have shown that a direct comparison of tissue clearance values expressed on a per gram body weight basis with urine flow rates in the presence of ANP enables an evaluation of the contribution of ANP to preferentially regulate plasma volume. Using this criterion, we demonstrated that even though skeletal muscle has the largest extravascular space into which plasma proteins can exchange, and the microvasculature of skeletal muscle appears to be one of the more responsive organs to ANP modulation of vascular permeability, it may contribute less than 30% of the overall exchange capacity required for ANP to preferentially regulate plasma volume. On

the other hand, the combined response of skeletal muscle and skin may account for 80 to 90% of that required for regulation of vascular volume by ANP-dependent permeability regulation. Further, the action of ANP to increase vascular permeability in colon, jejunum and duodenum appears to be one likely mechanism for further regulation of vascular volume via action of ANP on both renal water and salt excretion and increased vascular permeability. Refinement of two-tracer methods for application in other tissues and further application of MR imaging techniques to enable paired measurements of control and ANP responses on the same animal are needed to evaluate these questions.

Appendix 1

Criterion for no increase in plasma protein concentration (C_p) when ANP increases both urine flow and vascular permeability (i.e. that the rate of change of plasma protein concentration, dC_p/dt, is zero during ANP administration) are below:By definition

$$C_p = M/V_p$$

where M is the mass of protein in the plasma volume, V_p. Therefore

$$dC_p/dt = (1/V_p)(dM/dt) - \left(M/V_p^2\right)(dV_p/dt).$$

For the criterion that $dC_p/dt = 0$, we have

$$(1/V_p)(dM/dt) = \left(M/V_p^2\right)(dV_p/dt).$$

At $t = 0$,

$$dM/dt = \text{Clearance} \times C_p(0) \text{ and } M = V_p(0) \times C_p(0).$$

If urine excretion rate is U and fluid flow from blood to tissue is J_v, then

$$dV_p/dt = U + J_v$$

Thus

$$dC_p/dt = 0$$

when

$$\text{Clearance} \times (C_p(0)/V_p(0)) = (U + J_v)(C_p(0)/V_p(0))$$

As $(C_p(0)/V_p(0))$ is common to both sides of the equality,

$$\text{Clearance} = U + J_v.$$

The above derivation makes no assumptions about the mechanism of protein movement (i.e. the relative contributions of solvent drag and diffusion to albumin clearance are not specified). However, the above relation allows an estimate of J_v. The maximum contribution of solvent drag to the albumin clearance would then equal $J_v \times C_p$, when the solvent drag reflection coefficient is assumed to be close to zero.

Appendix 2

Derivation of relations to estimate apparent macromolecule permeability coefficients

Estimate of apparent permeability coefficient P_s from slope/step analysis. We use the signal intensity trace in Fig. 4*C* to illustrate the principle.

The early part of the trace is divided into two regions: step increase in intensity above baseline and the initial rate of increase of intensity following this step as the additional tracer accumulates in the region of interest (ROI).

Assuming signal intensity is proportional to the total amount of tracer in the ROI:

Step measures the amount of tracer that fills the vascular space in the ROI $= V_p \times C_p$ where V_p is the intravascular volume in the ROI and C_p is the tracer concentration in the plasma.

Slope measures: (total amount of tracer in tissue at time ΔT) $-$ (amount of tracer in vascular space at time T_0)$/\Delta T$. This is equal to the flux of tracer into tissue (J_s) across surface area for exchange (S) in the ROI.

Thus

$$\text{slope/step} = J_s/V_pC_p \text{ and}$$

because $P_s = (J_s/S)/(C_p)$ (assuming tissue concentration initially is zero),
$P_s = (\text{slope/step}) \times (V/S)$ where V/S is the ratio of plasma volume to surface area for exchange in the ROI.

For single perfused microvessels assumed to be cylindrical, V/S is equal to $r/2$ where r is the microvessel radius and

$P_s = (\text{slope/step}) \times r/2$ (Adamson *et al.* 1988).

To apply the step/slope analysis for the signal intensity measured from an ROI defined in an MR image containing no large vessels, V/S was assumed to be determined by a population of microvessels ranging in size from 5 μm diameter capillaries ($r/2 = 1.25$ μm) to 30 μm diameter venules ($r/2 = 7.5$ μm). If capillaries and venules contribute equal exchange areas, a mean $r/2$ is 4.4×10^{-4} cm. The estimate of $r/2$ is smaller if capillaries contribute proportionally more exchange area.

Two-tracer methods

The tissue clearance is equal to tracer mass M accumulated across area S of microvascular surface in time T/C_p where C_p is mean plasma protein concentration.
Thus, Clearance $\times$ $C_p = J_s$ across Area S.Because $P_s = (J_s/S)/(C_p - C_t)$, C_t is concentration of plasma protein in extravascular tissue space.

$$P_s = [\text{Clearance} \times C_p)/S]/(C_p - C_t).$$

The unknown in this calculation is always the value of exchange surface area S. However, when the local

intravascular volume is measured as in this case (5 min tracer volume), a reasonable first approximation is to assume that the intravascular volume is related to the surface area in the small tissue sample via a mean volume to surface ratio. We used the same value for these tracer analyses as used for the MRI tracer approach described above.
Thus

$$P_s = ([\text{Clearance} \times C_p)/V_p][S/V_p])/(C_p - C_t)$$
$$= (\text{Clearance}/V_p)(r/2)$$

when $C_p \gg C_t$, $(C_p - C_t) = C_p$ and V_p/S can be approximated by a mean volume to surface ratio of 4.4×10^{-7} cm.

Note when clearances are expressed as a plasma equivalent volume measured over 30 min (1800 s) as in Figs 1 through 3, the above relation is equal to

$$P_s = [(\text{Normalised 30 min Clearance}]/1800)] \times r/2.$$

The error in the estimate of $r/2$ is expected to be much smaller than errors in the estimate of surface area, especially when an agent acts mainly to increase permeability and there is not a large change in perfusion conditions.

Contribution of solvent drag to blood-to-tissue exchange

The apparent permeability coefficient P_s defined above as $(J_s/S)/(C_p - C_t)$ measures a true diffusion permeability coefficient only when there is no solvent drag, i.e.

$$J_s/S = P_s\,(C_p - C_t)$$

explained in detail elsewhere (Curry, 1984; McKay & Huxley, 1995). If ANP also increases the blood to tissue water flux, J_v, then the blood to tissue flux of albumin is larger and

$$J_s/S = P_s\,(C_p - C_t) + J_v\,(1 - \sigma)\,C_p$$

where σ is the solvent drag reflection coefficient. When $C_p \gg C_t$, $(J_s/S)/C_p = P_s + J_v(1 - \sigma)$. McKay and Huxley show that the contribution of the solvent drag term $J_v(1 - \sigma)$ may be significant because J_v is increased in the presence of ANP (McKay & Huxley, 1995).

References

Adamson RH, Huxley VH & Curry FE (1988). Single capillary permeability to proteins having similar size but different charge. *Am J Physiol Heart Circ Physiol* **254**, H304–H312.

Almeida FA, Suzuki M & Maack T (1986). Atrial natriuretic factor increases hematocrit and decreases plasma volume in nephrectomized rats. *Life Sci* **39**, 1193–1199.

Brekke C, Lundervold A, Enger PO, Brekken C, Stalsett E, Pedersen TB, Haraldseth O, Kruger PG, Bjerkvig R & Chekenya M (2006). NG2 expression regulates vascular morphology and function in human brain tumours. *Neuroimage* **29**, 965–976.

Brookes ZL & Kaufman S (2005). Effects of atrial natriuretic peptide on the extrasplenic microvasculature and lymphatics in the rat *in vivo*. *J Physiol* **565**, 269–277.

Curry FE (1984). Mechanics and thermodynamics of transcapillary exchange. In *Handbook of Physiology*, section 2, *The Cardiovascular System*, vol IV, *Microcirculation,* ed. Renkin EM & Michel CC, pp. 375–409. American Physiological Society, Bethesda, MD.

Curry FE, Huxley VH & Adamson RH (1983). Permeability of single capillaries to intermediate-sized coloured solutes. *Am J Physiol Heart Circ Physiol* **245**, H495–H505.

Curry FR (2005). Atrial natriuretic peptide: an essential physiological regulator of transvascular fluid, protein transport, and plasma volume. *J Clin Invest* **115**, 1458–1461.

Drummond GB (2009). Reporting ethical matters in *The Journal of Physiology*: standards and advice. *J Physiol* **587**, 713–719.

Hamza SM & Kaufman S (2009). Role of spleen in integrated control of splanchnic vascular tone: physiology and pathophysiology. *Can J Physiol Pharmacol* **87**, 1–7.

Huxley VH, Curry FE & Adamson RH (1987). Quantitative fluorescence microscopy on single capillaries: α-lactalbumin transport. *Am J Physiol Heart Circ Physiol* **252**, H188–H197.

Kishimoto I, Dubois SK & Garbers DL (1996). The heart communicates with the kidney exclusively through the guanylyl cyclase-A receptor: acute handling of sodium and water in response to volume expansion. *Proc Natl Acad Sci U S A* **93**, 6215–6219.

Lopez MJ, Garbers DL & Kuhn M (1997). The guanylyl cyclase-deficient mouse defines differential pathways of natriuretic peptide signalling. *J Biol Chem* **272**, 23064–23068.

McKay MK & Huxley VH (1995). ANP increases capillary permeability to protein independent of perfusate protein composition. *Am J Physiol Heart Circ Physiol* **268**, H1139–H1148.

Michel CC & Curry FE (1999). Microvascular permeability. *Physiol Rev* **79**, 703–761.

Misselwitz B, Schmitt-Willich H, Ebert W, Frenzel T & Weinmann HJ (2001). Pharmacokinetics of Gadomer-17, a new dendritic magnetic resonance contrast agent. *MAGMA* **12**, 128–134.

Nagy JA, Benjamin L, Zeng H, Dvorak AM & Dvorak HF (2008). Vascular permeability, vascular hyperpermeability and angiogenesis. *Angiogenesis* **11**, 109–119.

Nedrebo T, Reed RK & Berg A (2003). Effect of α-trinositol on interstitial fluid pressure, edema generation, and albumin extravasation after ischemia-reperfusion injury in rat hind limb. *Shock* **20**, 149–153.

Renkin EM & Tucker V (1996). Atrial natriuretic peptide as a regulator of transvascular fluid balance. *News Physiol Sci* **11**, 138–143.

Renkin EM & Tucker VL (1998). Measurement of microvascular transport parameters of macromolecules in tissues and organs of intact animals. *Microcirculation* **5**, 139–152.

Sabrane K, Kruse MN, Fabritz L, Zetsche B, Mitko D, Skryabin BV, Zwiener M, Baba HA, Yanagisawa M & Kuhn M (2005). Vascular endothelium is critically involved in the hypotensive and hypovolemic actions of atrial natriuretic peptide. *J Clin Invest* **115**, 1666–1674.

Sarelius IH & Huxley VH (1990). A direct effect of atrial peptide on arterioles of the terminal microvasculature. *Am J Physiol Regul Integr Comp Physiol* **258**, R1224–R1229.

Sarelius IH, Kuebel JM, Wang J & Huxley VH (2006). Macromolecule permeability of in situ and excised rodent skeletal muscle arterioles and venules. *Am J Physiol Heart Circ Physiol* **290**, H474–H480.

Schreier B, Borner S, Volker K, Gambaryan S, Schafer SC, Kuhlencordt P, Gassner B & Kuhn M (2008). The heart communicates with the endothelium through the guanylyl cyclase-A receptor: acute handling of intravascular volume in response to volume expansion. *Endocrinology* **149**, 4193–4199.

Trippodo NC & Barbee RW (1987). Atrial natriuretic factor decreases whole-body capillary absorption in rats. *Am J Physiol Regul Integr Comp Physiol* **252**, R915–R920.

Tucker VL, Simanonok KE & Renkin EM (1992). Tissue-specific effects of physiological ANP infusion on blood-tissue albumin transport. *Am J Physiol Regul Integr Comp Physiol* **263**, R945–R953.

Author contributions

F.E.C., R.K.R., H.W., M.K., C.B.R. and R.H.A. contributed to the conception and design of experiments. C.B.R., F.E.C., F.T., T.K., B.G., I.M. and O.T. contributed to the execution of experiments. J.F.C., K.L., R.H.A., F.E.C., R.K.R., H.W., C.B.R. and M.K. contributed to the analysis and interpretation of experiments. F.E.C. wrote the initial draft of the manuscript and M.K., R.K.R., R.H.A., H.W., C.B.R. and J.F.C. contributed to writing and revising the manuscript. The MRI and isotope experiments were carried out in Bergen; the KO mice were developed in Würzburg. All authors approved the final version of the manuscript.

Acknowledgements

We greatly appreciate the technical assistance of Gerd Salvesen and financial support from NIH HL28607, Deutsche Forschungsgemeinschaft SFB 688, and the Research Council of Norway.